PCT

INTERNATIONAL SEARCH REPORT

(PCT Article 18 and Rules 43 and 44)

Applicant's or agent's file reference	FOR FURTHER ACTION	see Notification of Transmittal of International Search Report (Form PCT/ISA/220) as well as, where applicable, item 5 below
12970/WO/01		
International application No	International filing date *(day/month/year)*	(Earliest) Priority Date *(day/month/year)*
PCT/IL 03/01086	18/12/2003	19/12/2002

Applicant

RAFAEL-ARMAMENT DEVELOPMENT AUTHORITY LTD.

This International Search Report has been prepared by this International Searching Authority and is transmitted to the applicant according to Article 18. A copy is being transmitted to the international Bureau

This International Search Report consists of a total of 5 sheets

[X] It is also accompanied by a copy of each prior art document cited in this report.

1. **Basis of the report**

   a. With regard to the **language**, the international search was carried out on the basis of the international application in the language in which it was filed, unless otherwise indicated under this item

   [ ] the international search was carried out on the basis of a translation of the international application furnished to this Authority (Rule 23.1(b)).

   b. With regard to any **nucleotide and/or amino acid sequence** disclosed in the international application, the international search was carried out on the basis of the sequence listing :

   [ ] contained in the international application in written form.

   [ ] filed together with the international application in computer readable form

   [ ] furnished subsequently to this Authority in written form.

   [ ] furnished subsequently to this Authority in computer readble form.

   [ ] the statement that the subsequently furnished written sequence listing does not go beyond the disclosure in the international application as filed has been furnished

   [ ] the statement that the information recorded in computer readable form is identical to the written sequence listing has been furnished

2. [ ] **Certain claims were found unsearchable** (See Box I).

3. [ ] **Unity of invention is lacking** (see Box II).

4. With regard to the title,

   [X] the text is approved as submitted by the applicant.

   [ ] the text has been established by this Authority to read as follows:

5. With regard to the **abstract**,

   [ ] the text is approved as submitted by the applicant.

   [X] the text has been established, according to Rule 38.2(b), by this Authority as it appears in Box III. The applicant may, within one month from the date of mailing of this international search report, submit comments to this Authority.

6. The figure of the drawings to be published with the abstract is Figure No. 4

   [ ] as suggested by the applicant.

   [X] because the applicant failed to suggest a figure

   [ ] because this figure better characterizes the invention.

   [ ] None of the figures.

Box III TEXT OF THE ABSTRACT (Continuation of item 5 of the first sheet)

A reconnaissance system that comprises a projectile (10) that has an opening (17) through which images of a target area can be acquired. The projectile (10) is launched from a portable launcher (30) towards the target area, and comprises image acquiring means (13,14) for acquiring images of the target area through the opening (17) and for transmitting the images to a remote station (70); means for stabilizing the projectile (10) and/or the image acquiring means (13,14) while flying in a nearly-parabolic trajectory above the target area; and a remote station (70), for receiving and displaying the transmitted images that comprises a monitor (71) for displaying the transmitted images.

A. CLASSIFICATION OF SUBJECT MATTER
IPC 7 F42B12/36 F41G3/14

According to International Patent Classification (IPC) or to both national classification and IPC

B. FIELDS SEARCHED

Minimum documentation searched (classification system followed by classification symbols)
IPC 7 F41G F42B

Documentation searched other than minimum documentation to the extent that such documents are included in the fields searched

Electronic data base consulted during the international search (name of data base and, where practical, search terms used)
EPO-Internal, WPI Data, PAJ

C. DOCUMENTS CONSIDERED TO BE RELEVANT

Category *	Citation of document, with indication, where appropriate, of the relevant passages	Relevant to claim No.
X	US 6 056 237 A (WOODLAND RICHARD L K) 2 May 2000 (2000-05-02) column 3, line 28 - line 34 column 3, line 60 -column 4, line 7 column 7, line 15 - line 38 column 8, line 27 - line 37 column 10, line 46 - line 49 column 11, line 19 - line 30 column 13, line 33 - line 41 column 13, line 63 -column 14, line 7 column 14, line 31 - line 58 figures 1,2,7,21,26-31 abstract	1-10, 12-18
Y	---	11
	-/--	

[X] Further documents are listed in the continuation of box C

[X] Patent family members are listed in annex

* Special categories of cited documents :

"A" document defining the general state of the art which is not considered to be of particular relevance

"E" earlier document but published on or after the international filing date

"L" document which may throw doubts on priority claim(s) or which is cited to establish the publication date of another citation or other special reason (as specified)

"O" document referring to an oral disclosure, use, exhibition or other means

"P" document published prior to the international filing date but later than the priority date claimed

"T" later document published after the international filing date or priority date and not in conflict with the application but cited to understand the principle or theory underlying the invention

"X" document of particular relevance; the claimed invention cannot be considered novel or cannot be considered to involve an inventive step when the document is taken alone

"Y" document of particular relevance; the claimed invention cannot be considered to involve an inventive step when the document is combined with one or more other such documents, such combination being obvious to a person skilled in the art.

"&" document member of the same patent family

Date of the actual completion of the international search	Date of mailing of the international search report
8 April 2004	19/04/2004

Name and mailing address of the ISA	Authorized officer
European Patent Office, P B 5818 Patentlaan 2 NL - 2280 HV Rijswijk Tel. (+31-70) 340-2040, Tx 31 651 epo nl, Fax: (+31-70) 340-3016	Gex-Collet, A-L

C.(Continuation) DOCUMENTS CONSIDERED TO BE RELEVANT

Category *	Citation of document, with indication, where appropriate, of the relevant passages	Relevant to claim No.
Y	DE 44 16 557 A (BODENSEEWERK GERAETETECH) 23 November 1995 (1995-11-23) column 2, line 52 - line 65 figures 1,2	11

Patent document cited in search report	Publication date	Patent family member(s)	Publication date
US 6056237 A	02-05-2000	NONE	
DE 4416557 A	23-11-1995	DE 4416557 A1	23-11-1995
		FR 2719920 A1	17-11-1995
		GB 2289389 A ,B	15-11-1995

6/172 A mechanical device for reducing the spin of a satellite consists of two masses m attached to wires or thin metal tapes which unwind when released and acquire additional angular momentum at the expense of the angular momentum of the satellite. The masses are then released when unwound. Each tape has a length $R\phi$ and is fastened to its point A. If the satellite is spinning at an initial speed ω_0 when the masses are released with $\beta = 0$, determine the rate $\dot{\beta}$ of unwinding and find the new angular velocity ω_n of the satellite when $\beta = \phi$. The moment of inertia of the satellite exclusive of the m's is I. (*Hint:* Equate the angular momentum and the kinetic energy of the system to their respective initial values.) *Ans.* $\dot{\beta} = \omega_0$ constant

$$\omega_n = \frac{I + 2mR^2(1 - \phi^2)}{I - 2mR^2(1 - \phi^2)}\omega_0$$

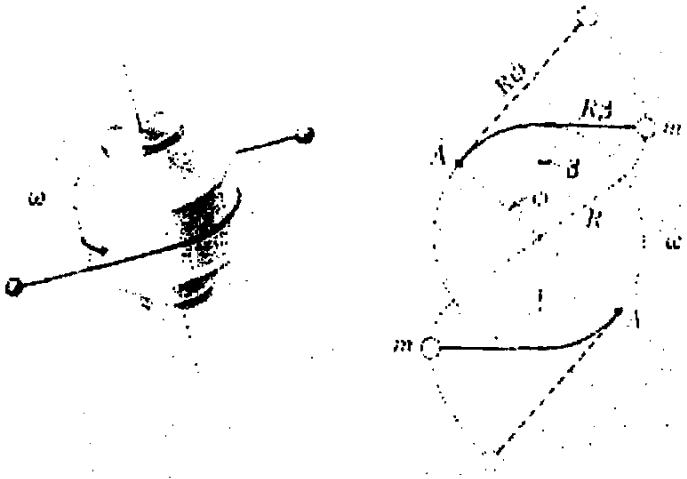

Problem 6/172

6/173 The two slender bars each having a mass of 4 kg are hinged at B and pivoted at C. If a horizontal impulse of $\int F\,dt = 14\ \text{N}\cdot\text{s}$ is applied to the end A of the lower bar during an interval of 0.1 s during which the bars are still essentially in their vertical rest positions, compute the angular velocity ω_2 of the upper bar immediately after the impulse. *Ans.* $\omega_2 = 2.50\ \text{rad/s}$

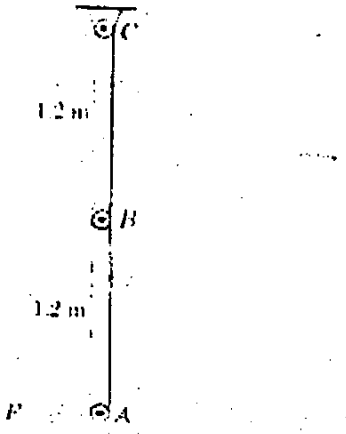

Problem 6/173

-Relevant extract from "Dynamics; 2nd Edition; J.L. Meriam and L.G. Kraige, John Wiley and Sons; 1987".

FOOTNOTE

In a recent private communication to the author Warren states that his definition of the characteristic overpressure can be somewhat generalised to be a little more embracing. The suggested definition is now

$$\Delta P = \frac{4}{T}[I_{MAX} - I_{MIN}]$$

I is now the running integral of the overpressure, I_{MAX} is its maximum value and I_{MIN} is the minimum value if and only if I is somewhere negative. (That is I_{MIN} is either zero or negative.) In most cases I will not be negative

For the configurations considered in sections 5–9 the characteristic overpressures given by either definition are identical.

From the work reported in Refs 2, 3 and here it is readily seen that with the constraint given R (or P) the minimum value of $(I_{MAX} - I_{MIN})$ is again given by a Dirac function at $x=0$, so that $I_{MIN}=0$. Although of course negative values of I will lead to different values for the time signature, it does not seem likely that the new definition for the characteristic overpressure will lead to a different value for the lower bound value to that given by the definition as considered in this note.

Prediction of the lift and moment on a slender cylinder-segment wing-body combination

K. R. CROWELL* and C. T. CROWE†

Department of Mechanical Engineering, Washington State University

NOTATION

a_{-1}	residue of complex potential
a	real constant
a_1, a_2, a_3	complex constants
C_1, C_2, C_3	complex constants
C_L	lift coefficient
F	force
M	moment
m	doublet strength
r	radius of body
S	cross-sectional area
U	free stream velocity
w	complex potential of crossflow
x	spanwise co-ordinate
y	vertical co-ordinate
z	streamwise direction
α	angle of attack
δ	slenderness parameter
ϵ	complex variable defined by eqn. 12
ζ_1	complex variable in crossflow plane
ζ_2	complex variable defined by eqn. 9
ζ_3	complex variable defined by eqn. 10
η	complex constant
θ	angular location of doublet in ζ_3 plane
ξ_B	complex function for the body axis
ρ	free stream density
ϕ	perturbation velocity potential

Subscripts

B	base plane
x	spanwise direction
y	vertical direction
z	streamwise direction

Received 29th February 1972.

*Graduate Student.
†Associate Professor.

INTRODUCTION

The design of a vehicle with cruise capability which can be packaged in a volume limited space, such as a cylindrical tube, centres around the problem of folding the lifting and control surfaces in such a manner that their deployment is simple and reliable. Several folding schemes are illustrated in Fig. 1. A wing fabricated of a flexible material and suspended by lines from the fuselage (parawing, Fig. 1a) can be folded to occupy only a small volume. These wings, however, are difficult to deploy at high forward speeds and have characteristically poor lift/drag ratios[1] unsuitable for high performance cruise capability. Another concept which allows storing the wing in a volume-limited space is the "scissor" wing (Fig. 1b) which, when deployed, swings out from a cavity in the fuselage. Besides the difficulties associated with packaging the wings in the fuselage and designing a reliable hinge mechanism,

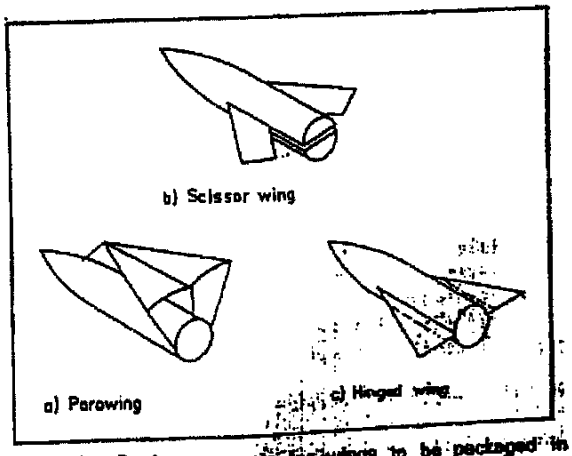

Figure 1 Design concepts for wings to be packaged in volume-limited systems.

there is the disadvantage of having a sizable cavity in the load-carrying section of the fuselage, compromising the vehicle's overall utility. A third technique is to hinge the wing (Fig. 1c) such that it lies on the fuselage in its folded position. If the space between the fuselage and cylindrical constraint is small the wing's span is severely limited. Such a technique, however, can often be used to fold the control surfaces.

A novel wing design which can be easily hinged and packaged within a cylinder is shown in Fig. 2. In the folded position, the wing rests on the cylindrical fuselage. When deployed, the two semi-spans simply rotate about a hinge along the top of the fuselage and a wing consisting of two cylinder segments evolves. The purpose of this note is to present the results derived from slender-body theory for the lift and pitching moment on such a wing-body combination. Although the assumptions of slender-body theory may not always be fully realised for practical aircraft, the theory does provide a relatively simple technique to estimate effects due to configuration changes which would otherwise require much more elaborate calculations. In addition, the results of slender-body theory can be incorporated into more complete estimation methods[2].

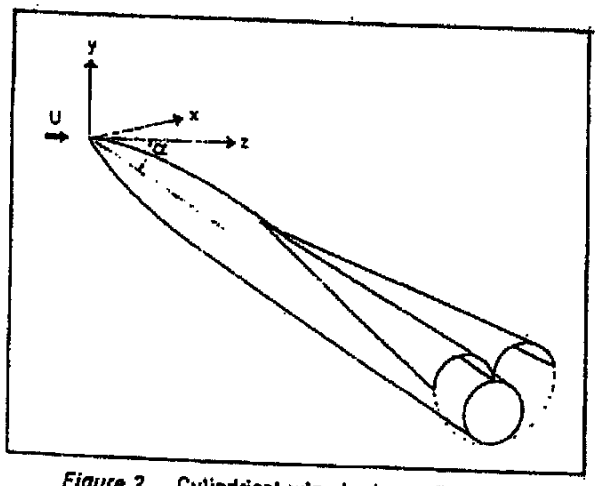

Figure 2. Cylindrical wing-body configuration.

A slender body is characterised by slowly changing cross-sectional dimensions in the streamwise direction such as a wing of low aspect ratio or a fuselage with a small thickness ratio. Expanding the velocity potential function in powers of a slenderness parameter (such as body thickness or aspect ratio) and retaining the lowest order terms reveals[3] that:

(*i*) At large distances from the slender body the flow becomes axisymmetric and equal to the flow around an axisymmetric body having the same cross-sectional area distribution as the actual slender body.

(*ii*) Near the body, the flow differs from that around the equivalent body of revolution by a two-dimensional constant-density cross-flow part that allows the tangency condition to be satisfied.

The solution for the flow field far from the body is known as the outer solution and that for the flow near the body as the inner solution.

Ward[1] shows that the complex lateral force acting on a pointed slender body is given by

$$F_z + iF_y = -\rho U^2 \int_{C_B} \phi d\zeta + 0(\delta^3 \log^2 \delta) \qquad (1)$$

where ϕ is the velocity potential and the line integral is evaluated at the base plane. Using the inner and outer solutions for the velocity potential Ward shows that eqn 1 reduces to

$$F_z + iF_y = \rho U^2 [2\pi i a_{-1}(z_B) + S'(z_B)\,\xi_s(z_B) + S(z_B)\,\xi_s'(z_B)] \qquad (2)$$

where $\xi_s(z)$ is a complex function for the centre of the body's cross-sectional area $S(z)$ and $a_{-1}(z)$ is the residue of the complex potential for the inner solution; that is, the constant-density crossflow. Ward also derives an expression for the complex moment about the nose of a slender body which is

$$M_x + iM_y = \rho U^2 \{2\pi i a_{-1}(z_B)\, z_B - 2\pi i \int_0^{z_B} a_{-1}(z)\, dz + i[S'(z_B)\,\xi_s(z_B) + S(z_B)\,\xi_s'(z_B)\, z_B - S(z_B)\,\xi_s(z_B)]\} \qquad (3)$$

The co-ordinate system used in this study is illustrated in Fig. 2. The lift is the force component in the positive y-direction and the pitching moment is about the x-axis. For the configuration of interest here there is no change in cross-sectional area at the base so

$$S'(z_B) = 0 \qquad (4)$$

Also, because the body has a rectilinear axis which is assumed to lie in the $y-z$ plane (no sideslip velocity) $\xi_s(z)$ becomes

$$\xi_s(z) = -i\alpha z \qquad (5)$$

where α is the angle of attack. Thus eqn. (2) for the lift force becomes

$$L = F_y = \rho U^2 [-2\pi i a_{-1}(z_B) - S(z_B)\,\alpha] \qquad (6)$$

and the pitching moment from eqn. (3) is

$$M_x = \rho U^2 [2\pi i a_{-1}(z_B)\, z_B - 2\pi i \int_0^{z_B} a_{-1}(z)\, dz] \qquad (7)$$

The distance of the centre of pressure from the nose is found by dividing the moment by the negative lift force.

The complex potential for the constant-density crossflow solution must yield a zero velocity at infinity and a velocity of $-\alpha$ at the body surface to satisfy the tangency condition. To solve for the crossflow complex potential, however, it is more straightforward to solve the problem assuming the body is at rest and immersed in a rectilinear flow parallel to the y-axis with velocity α at infinity. The residue obtained from such a solution is the same as that for the correct inner solution because the potentials differ only by an $i\alpha\zeta$ term.

The solution for the constant density crossflow can be found using conformal transformations with which the cross section is mapped onto a plane for which an elementary flow solution is possible. Consider the flow around the base plane, ζ_1, shown in Fig. 3a with

$$w = -i\alpha\zeta_1 \qquad (8)$$

at infinity. Applying the conformal transformation

$$\zeta_2 = 2i\pi r/\zeta_1 + \pi \qquad (9)$$

the configuration becomes that shown in 3b where the body becomes an infinite wall and the semi-spans become two semi-infinite slits. The uniform flow at infinity transforms into a doublet located at $x_2 = \pi$ and directed along the positive x_2 axis. Utilising the following form of a Schwartz-Christoffel transformation,

$$\zeta_3 = a(\zeta_2 + 1)/\sqrt{\zeta_2} + 2\log(\sqrt{\zeta_2 + 1}/\sqrt{\zeta_2 - 1}) + i\pi \qquad (10)$$

where $a = 0{\cdot}5269$, the flow in the ζ_2-plane transforms into a doublet near an infinite wall in the ζ_3-plane. The doublet,

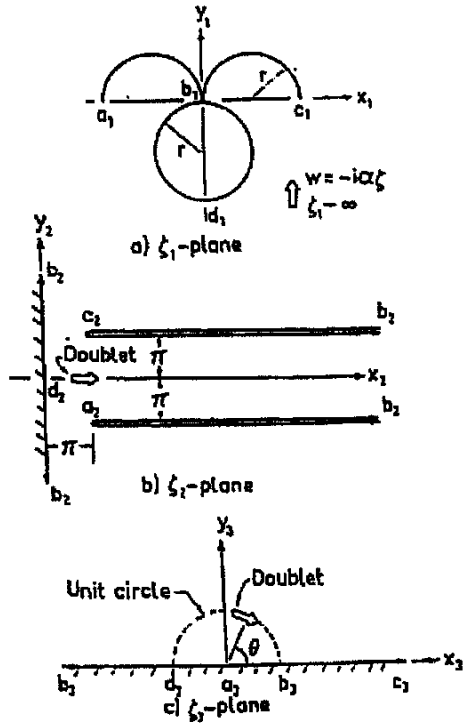

Figure 3. Conformal transformation of wing-body cross-section at the base plane into an infinite wall

which represents the uniform flow at infinity in the ζ_1-plane, lies on and is tangent to a unit circle centred at the origin of the ζ_3-plane. Replacing the wall by another doublet, the complex potential in the ζ_3-plane is found to be

$$w(\zeta_3) = 2m \sin\theta \left[\frac{\zeta_3}{(\zeta_3 - e^{i\theta})(\zeta_3 - e^{-i\theta})}\right] \quad . \quad . \quad . \quad (11)$$

where m is the doublet strength and θ is the angular location of the doublet on the unit circle. As the wing span is truncated, corresponding to stations forward of the base plane, the slits in the ζ_2-plane move away from the wall and doublet while, in the ζ_3-plane, the doublet moves along the unit circle toward the y_3-axis. In the limit of no wing, the doublet in the ζ_3-plane is on the y_3-axis, directed parallel to the x_3-axis and yields the complex potential for the flow past a cylinder in the ζ_1-plane.

As discussed above the lift and pitching moment can be evaluated from the residue of the Laurent series for $w(\zeta_1)$. This residue can be determined by evaluating the flow near the doublet in the ζ_3-plane and relating ζ_3 to ζ_1. Substituting

$$\zeta_3 = \eta + \epsilon, \quad . \quad . \quad . \quad . \quad (12)$$

where $\eta = e^{i\theta}$, into eqn. (11) and expanding for

$$0 < |\epsilon| < 1,$$

one obtains

$$\frac{w}{2m} = \frac{-ie^{i\theta}}{2\epsilon} + \frac{e^{-i\theta}}{4\sin\theta} \sum_{k=0}^{\infty} \left(\frac{i\epsilon}{2\sin\theta}\right)^k \quad . \quad (16)$$

Combining eqn. (12) and the transformation eqns. (9) and (10) the following asymptotic relation between ϵ and ζ_1 results

$$2i\pi r/\zeta_1 = a_1\epsilon + a_2\epsilon^2 + a_3\epsilon^3 + 0(\epsilon^4) \quad . \quad . \quad (14)$$

where

$$a_1 = \frac{a(\eta-1)}{2\eta^{3/2}} - \frac{2}{\eta^{1/2}(\eta-1)}$$

$$a_2 = \frac{a(3-\eta)}{8\eta^{3/2}} + \frac{3\eta-1}{2\eta^{3/2}(\eta-1)^2}$$

$$a_3 = \frac{a(\eta-5)}{16\eta^{7/2}} - \frac{15\eta^2-10\eta+3}{12\eta^{5/2}(\eta-1)^3}$$

Inverting eqn. (14) for $\epsilon = \epsilon(\zeta_1)$, that is

$$\epsilon = C_1/\zeta_1 + C_2/\zeta_1^2 + C_3/\zeta_1^3 + \quad . \quad . \quad . \quad (15)$$

where

$$C_1 = 2\pi i r/a_1$$

$$C_2 = 4a_2\pi^2 r^2/a_1^3$$

$$C_3 = 8i\pi^3 r^3 (a_2a_1 - 2a_2^2)/a_1^5$$

and substituting into eqn. (13) gives the following asymptotic expansion for w as $\zeta_1 \to \infty$

$$w(\zeta_1) = -i\alpha\zeta_1 + \alpha\left[\frac{iC_2}{C_1} + \frac{C_1 e^{-i\theta}}{2\sin\theta}\right] + \frac{i\alpha}{\zeta_1}\left[\frac{C_1C_2 - C_2^2}{C_1^2} + \frac{C_1^2 e^{-2i\theta}}{4\sin^2\theta}\right] \quad . \quad . \quad (16)$$

where the doublet strength in the ζ_3-plane was chosen to satisfy $w(\zeta_1) \to -i\alpha\zeta_1$ as $\zeta_1 \to \infty$. Finally the residue becomes

$$a_{-1} = i\alpha\pi^2 r^2 \left\{\left[\frac{\sin\theta/2}{a\sin^2\theta/2+1}\right]^4 \left[\frac{a}{6}\left(\frac{9\cos^2\theta/2-4}{\sin^3\theta/2}\right) - \frac{1}{4}a^2(\sin^2\theta/2+1) - \frac{1}{12}\left(\frac{3\sin^2\theta/2-1}{\sin^4\theta/2}\right)\right] + \frac{\sin^2\theta/2}{\sin^2\theta\,(a\sin^2\theta/2+1)^2}\right\} \quad . \quad (17)$$

For the crossflow at the base, for which $\theta = 70\text{-}86°$, the residue has the value

$$a_{-1} = 0.296\,\alpha\pi^2 r^2 l \quad . \quad . \quad . \quad (18)$$

which when used in eqn. (6) results in a lift coefficient of

$$C_L = 1.90\Lambda\alpha \quad . \quad . \quad (19)$$

and a lift curve slope of

$$C_{L_\alpha} = 1.90\Lambda \quad . \quad . \quad . \quad (20)$$

where Λ is the aspect ratio. Thus the lift curve slope of the cylinder-segment wing-body combination is 50% higher than that for a conventional mid-wing configuration.

In order to compare the lift and aerodynamic centre location of the semi-cylinder wing with other designs of the same span, a series of calculations were performed for the wing-body combinations illustrated in the table. The planform of each combination is identical. Each wing has a delta planform, a span twice the body diameter and an aspect ratio of unity based on the projected area. The forebody consists of a parabola of revolution with a 30° included angle at the nose. The wing begins at the junction of the forebody and cylindrical afbody. The centre of pressure, which according to linearised slender body theory, is the aerodynamic centre, was determined by evaluating the pitching moment about the nose and dividing by the negative value of lift force. The analysis for the high wing design is based on the work of Barlett[5] and the midwing results derive from Spreiter's[6] analysis.

It is noted from the table that the lift curve slope for the cylinder-segment wing is 35% higher than that for the high-wing design and 50% higher compared to the midwing configuration. One notes also that the aero-

TABLE

Comparison of lift curve slope and aerodynamic centre location for three wing-body configurations.

Plan View	Base Cross Section	C_{L_α}	z_{AC}/z_B
	Cylinder-Segment Wing	1.90	.781
	High-Wing	1.41	.755
$\Lambda=1$	Mid-Wing	1.27	.775

dynamic centre of the cylinder-segment wing is rearward of the high-wing aerodynamic centre because the lift distribution is concentrated in the region where the cylinders effect a reverse flow, i.e., near the trailing edge.

One disadvantage of the cylindrical wing concept is the limited span available (2 times body diameter). However, if the vehicle's forward velocity is such that the limited span is sufficient, the relatively high lift curve slope of the cylinder-segment wing makes it attractive for high performance designs.

A characteristic feature of the flow over low aspect ratio wings which has not been accounted for in the present analysis is leading edge separation. In any real situation, the flow will separate from the leading edges and form two spiral vortex sheets which roll up above the wing. In the case of the cylinder-segment wing, the geometry of these vortex sheets will be quite complex due to the rather complicated shape of the leading edge. The vortex sheets produce a definite contribution to the total lift force causing the actual lift to be somewhat higher than that predicted by slender body theory. This vortex lift contribution decreases with increasing Mach number and increases with increasing angle of attack. Analytical methods have been developed[7, 8] to predict the vortex lift on slender delta wings. However, additional studies are necessary in order to determine whether such methods can be successfully adapted to the cylinder-segment wing.

Experimental studies are currently in progress to investigate the validity of theory presented here.

REFERENCES

1. Ormiston, R. A. Theoretical and experimental aerodynamics of the sailwing. *Journal of Aircraft*. Vol 8, No 2, p 77–84 (1971).
2. Pitts, W. C., Nielsen, J. N., Kaattari, G. E. Lift and center of pressure of wing-body-tail combinations at subsonic speeds. NACA Rept 1307 (1957).
3. Ashley, H. and Landahl, M. T. *Aerodynamics of Wings and Bodies*. Addison-Wesley Pub Co. (1965).
4. Ward, G. N. *Linearised Theory of High Speed Flow*. Cambridge University Press (1955).
5. Bartlett, R. S. Slender body theory calculations of the effect on lift and moment of mounting the wing off the fuselage centre-line. ARC 25965, CP 830 (1964).
6. Spreiter, J. R. The aerodynamic forces on slender plane- and cruciform-wing and body combination. NACA Report 962 (1950).
7. Pachamus, E. C. Predictions of vortex lift characteristics by a leading-edge suction analogy. *Journal of Aircraft*. Vol 8, No 4, p 193–199 (1971).
8. Smith, J. H. B. Improved calculations of leading-edge separation from slender delta wings. TR 66070, Royal Aircraft Establishment (1966).

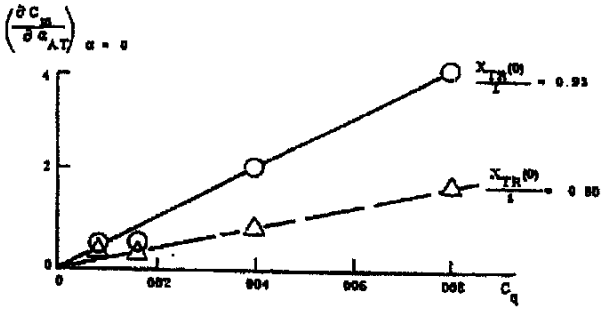

Fig. 5 Incremental blowing-induced stability derivative at $\alpha = 0$ as a function of blowing rate.

shown to exist in the α-range $\alpha_{AT} < \alpha < 4°$ for $\alpha_{AT} = 0°$, 1°, and 2° also would exist for other intermediate α_{AT}-values. It is hard to visualize any flow phenomenon that would invalidate this assumption. On the other hand, the local slopes used at $\alpha = \alpha_{AT}$ in obtaining the original fairing imply that $\partial C_m/\partial \alpha_{AT} = \partial C_m/\partial \alpha$; i.e., the transition movement derivative is assumed to be zero, $\partial x_{TR}/\partial \alpha = 0$, contrary to experimental evidence.[11]

Carpet-plotting the data[3] also for the other blowing rates gives the results shown in Fig. 4. At all blowing rates the destabilizing effect of asymmetric blowing is largest at small angles of attack near $\alpha_{AT} = 0$. One notices with some concern that the $C_m(\alpha)$-slope is negative for zero blowing rate, contrary to the measured effect of "free" asymmetric transition on a smooth solid model.[2] The reason for this anomaly is the "breathing" through the porous skin. It has been found that a porous skin model has substantially less C_{N_α} than a solid model,[6,7] an effect that can be visualized to result from reduced streamline displacement due to in-flow through the high pressure side of the porous skin model. Here, in the case of the asymmetric porous skin configurations for $\alpha_{AT} = 1°$ and $\alpha_{AT} = 2°$, this would mean that the porous skin side is less effective in displacing the freestream and, as a consequence, a loss of leeside-to-windward-side pressure differential results. The associated gain in aft body normal force explains the statically stabilizing effect of asymmetric porous skin geometry shown in Fig. 4 for $C_{m_q} = 0$.

The incremental effects of blowing on the static stability derivative C_{m_α} at $\alpha = 0$, obtained from Fig. 4 for $X_{TR}(0)/l = 0.93$, are shown in Fig. 5. Also shown are the data for the other aft body asymmetric blowing configuration tested, i.e., $X_{TR}(0)/l = 0.80$. The results indicate that the destabilizing effect of asymmetric aft body blowing increases linearly with the blowing rate, and that the effect decreases in magnitude when the mean transition point, $X_{TR}(0)/l$, moves forward towards the center of gravity, $X_{CG}/l = 0.60$, all in agreement with the theoretical and experimental results shown in Ref. 2.

References

[1] Martellucci, A. and Neff, R. S., "The Influence of Asymmetric Transition on Re-Entry Vehicle Motion," *Journal of Spacecraft and Rockets*. Vol. 8, No. 5, May 1971, pp. 476–482.

[2] Ericsson, L. E., "Transition Effects on Slender Vehicle Stability and Trim Characteristics," *Journal of Spacecraft and Rockets*. Vol. 11, No. 1, Jan. 1974, pp. 3–10.

[3] Martellucci, A., "Asymmetric Transition Effects on the Static Stability and Motion History of a Slender Vehicle," SAMSO TR-70-141, 1970, Space and Missiles Systems Organization, Los Angeles Air Force Base, Calif.

[4] Reding, J. P. and Ericsson, L. E., "Dynamic Support Interference," *Journal of Spacecraft and Rockets*. Vol. 9, No. 7, July 1972, pp. 547–553.

[5] Eckstrom, D. J., "The Influence of Mass and Momentum Transfer on the Static Stability and Drag of a Slender Cone—An Experimental Correlation," LMSC/D051269, July 1968, Lockheed.

[6] Wimberly, C. R., McGinnis, F. K., III, and Bertin, J. J., "Transpiration and Film Cooling Effects for a Slender Cone in Hypersonic Flow," *AIAA Journal*. Vol. 8, No. 6, June 1970, pp. 1032–1038.

[7] Ericsson, L. E. and Guenther, R. A., "Dynamic Instability Caused by Forebody Blowing," *AIAA Journal*. Vol. 11, No. 2, Feb. 1973, pp. 231–233.

[8] Bertin, J. J., McCloskey, M. H., Stalmach, C. J., and Wright, R. L., "Effect of Mass-Addition Distribution and Injectant on Heat Transfer and Transition Criteria," AIAA Paper 72-183, San Diego, Calif., 1972.

[9] Jecmen, D. M., Reding, J. P., and Ericsson, L. E., "An Application of Automatic Carpet Plotting to Wind-Tunnel Data Reduction," *Journal of Spacecraft and Rockets*. Vol. 4, No. 3, March 1967, pp. 408–410.

[10] Jecmen, D. M., "Automatic Carpet Plotting," LMSC 80563, Jan. 1967, Lockheed Missiles & Space Co., Sunnyvale, Calif.

[11] Ericsson, L. E., "Correlation of Attitude Effects on Slender Vehicle Transition," *AIAA Journal*. Vol. 12, No. 4, April 1974.

Cylindrical Wing-Body Configurations for Space-Limited Applications

D. E. Swanson* and C. T. Crowe†
Washington State University, Pullman, Wash.

Nomenclature

a_{-1} = residue
b = wing span
C_L = coefficient of lift
L = lift force
r = body radius
S = cross-sectional area
U_∞ = freestream velocity
V_n = normal component of velocity
w = complex potential
x, y = abscissa and ordinate in crossflow plane, respectively
Y = side force
z = streamwise coordinate
Z = complex variable in crossflow plane
Z_w = location of the wing in the Z_3-plane
α = angle of attack
γ = vortex strength distribution
ζ = distance along vortex sheet
Λ = aspect ratio
ξ = complex function for the body axis
ρ = freestream density

Subscripts

1, 2, 3 = first, second, and third complex planes
B = base plane of vehicle
∞ = freestream

Introduction

THE design of a vehicle with cruise capability which can be stored in a limited space usually involves the use of lifting surfaces which can be hinged or folded to satisfy the volume constraint. Several concepts for hinged and foldable wings are well-known. One such concept is the "scissor wing" which is hinged about its leading edge and swings out from a cavity in the fuselage. The primary disadvantage of this design is the reduction in load-carrying capacity and over-all utility of the vehicle due to the cavity in the fuselage. Another concept is the parawing, which is a flexible wing suspended by lines from

Received June 25, 1973; revision received September 10, 1973.
Index category: LV/M Aerodynamics.

* Graduate Student, Master's degree, Department of Mechanical Engineering.
† Associate Professor, Department of Mechanical Engineering.

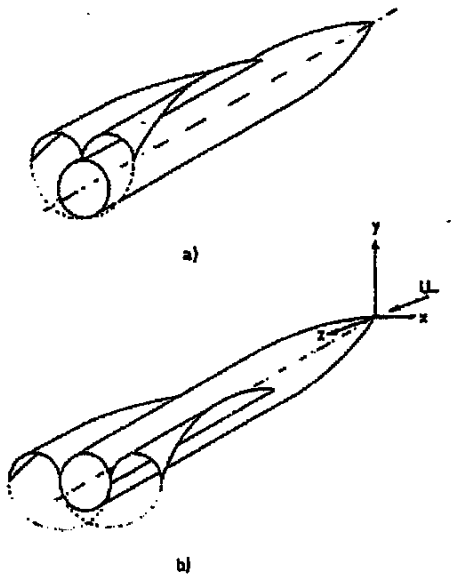

Fig. 1 Cylindrical wing-body configurations.

the fuselage. The parawing is difficult to deploy at high speeds and has a characteristically poor lift-drag ratio precluding high performance cruise operation. A third design possibility features flat wings hinged near the fuselage which, in the folded position, rest against the surface of the fuselage. The disadvantage of this particular design is the limited span available, especially if the vehicle is to be stored in a cylinder. The hinged wing, however, can be used effectively as a control surface. Another design[1] which has been proposed in connection with re-entry vehicles, consists of conical-shaped wings mounted on a half-cone fuselage. By mounting these wings on hinges at the fuselage, they can be folded against the fuselage to facilitate vehicle storage.

A promising design concept for hinged wings, studied by Crowell and Crowe,[2] is illustrated in Fig. 1a. The wings consist of two tapered semicylinders which hinge along the top of the fuselage. When not deployed, the two wings wrap around the side of the cylindrical fuselage. Theory predicts this wing-body configuration has a lift-curve slope 35% higher than that of a flat wing of the same span mounted on the top of the fuselage. Also, deployment is relatively simple and reliable. The major disadvantage is that the span is limited to twice the fuselage diameter and the lift developed may not satisfy design requirements.

The span and the attendant lift can be increased considerably by mounting the semicylindrical wings on the side of the fuselage as illustrated in Fig. 1b. In this case the span is three times the body diameter which, according to slender body theory, would result in a lift more than twice that obtained from the top-hinged wings at the same angle of attack. When not deployed the wings would wrap, one upon the other, around the underside of the fuselage. The purpose of this Note is to determine analytically the lift characteristics of such a wing-body configuration.

Analytic Approach

Slender body theory is used to predict the lift force. A slender body is characterized by small changes in cross-sectional area in the streamwise direction, such as a pointed slender fuselage or a low aspect-ratio wing. Expanding the velocity potential in powers of a slenderness parameter (such as body thickness or aspect ratio) and retaining the lowest order terms, Ward[3] shows that: 1) The flow at infinity for any general slender body becomes axisymmetric and equal to the flow at infinity around an equivalent axisymmetric body of revolution; and 2) Near the slender body, the flow differs from that around the equivalent body of revolution by a two-dimensional constant density crossflow part that makes the tangency condition satisfied. Thus, the flowfield at any section along the body can be subdivided into a velocity component parallel to the body axis and a crossflow component which can be treated as a two-dimensional ideal flow.

Ward[3] shows that the lift and side force on a slender body is obtained from

$$Y+iL=-i\rho U_\infty^2\int_{C_B} w(Z)\,dZ+\rho U_\infty^2[\xi'(z_B)S(z_B)+\xi(z_B)S'(z_B)] \quad (1)$$

where $w(Z)$ is the complex potential of the crossflow. The contour integral is evaluated at the station corresponding to the wing's maximum span (base plane). The variable $\xi(z)$ is a complex function for the center of the body's cross-sectional area, $S(z)$, with respect to the z-axis. $S'(z_B)$ is the rate of change of the body's cross-sectional area at the base plane which is zero for the wing-body configuration under study here. Evaluating the contour integral by the residue theorem, the equation for lift can be written as

$$L=\rho U_\infty^2\,Im[2\pi a_{-1}(z_B)-i\alpha S(z_B)] \quad (2)$$

where a_{-1} is the residue of the complex potential for the crossflow.

The tangency condition requires that the normal velocity component at the surface be equal to $\xi'(z_B)$, the velocity at infinity being zero. It is more straightforward, however, to let the normal velocity component be zero and the velocity at infinity be $-\xi'(z_B)$. The residue is the same for both cases.

The cross section of the wing-body configuration at the base plane is shown in Fig. 2a. It is assumed that the side-slip angle is zero so the flowfield at infinity is a rectilinear flow of magnitude α in the positive y-direction, the complex potential being $w=-i\alpha Z_1$. The flowfield can be constructed by representing the wings as vortex sheets. Then for each vortex on a wing, there must be a corresponding vortex of the opposite strength reflected inside the body to guarantee that the cylindrical fuselage is a streamline.

The analysis can be simplified by transforming the fuselage into a vertical slit using the transformation

$$Z_2=Z_1-(r^2/Z_1) \quad (3)$$

where r is the radius of the fuselage. The wings transform into near circular arcs connected to the body at the origin as shown in Fig. 2b. The complex potential at infinity remains unchanged. The flowfield can be solved in this plane by again representing the wings as symmetric vortex sheets, the fuselage automatically being a streamline by maintaining flow symmetry about the y-axis.

It was found, however, that the computation was facilitated by inverting the Z_2-plane onto a third plane

$$Z_3=1/Z_2 \quad (4)$$

The resulting configuration is shown in Fig. 2c. The fuselage is transformed into two slits along the y_3-axis, both extending to infinity. The wings becomes two slits which originate at $\pm 3/8r$ on